A SEARCH FOR IONOSPHERIC DISTURBANCES ASSOCIATED WITH PC 1 MICROPULSATIONS

Bruce Dingle

Stanford University

Prepared for:

Office of Naval Research
Advanced Research Projects Agency
National Science Foundation

March 1972

SU-SEL-72-021

A Search for Ionospheric Disturbances Associated with Pc 1 Micropulsations

by

Bruce Dingle

March 1972

Technical Report No. 3

Prepared for
Office of Naval Research

Sponsored by
National Science Foundation
Grant GA-17486 and
Defense Advanced Research Projects Agency
ARPA Order No. 1733

RADIOSCIENCE LABORATORY

STANFORD ELECTRONICS LABORATORIES

STANFORD UNIVERSITY · STANFORD, CALIFORNIA

Principal Investigator:

O.G. Villard, Jr.
(415) 321-2300

Scientific Officer:

Director, Field Projects Programs
Code 418
Office of Naval Research
Arlington, Virginia 22217

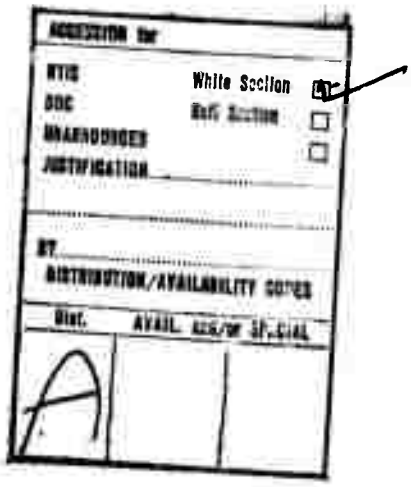

UNCLASSIFIED

Security Classification

DOCUMENT CONTROL DATA - R & D

(Security classification of title, body of abstract and indexing annotation must be entered when the overall report is classified)

1. ORIGINATING ACTIVITY (Corporate author)

Stanford Electronics Laboratories
Stanford University
Stanford, California 94305

2a. REPORT SECURITY CLASSIFICATION

UNCLASSIFIED

2b. GROUP

---

3. REPORT TITLE

A SEARCH FOR IONOSPHERIC DISTURBANCES ASSOCIATED WITH Pc 1 MICROPULSATIONS

4. DESCRIPTIVE NOTES (Type of report and inclusive dates)

Technical Report covering the period January 1971 through March 1972.

5. AUTHOR(S) (First name, middle initial, last name)

Bruce Dingle

6. REPORT DATE	7a. TOTAL NO. OF PAGES	7b. NO OF REFS
March 1972	68	9

8a. CONTRACT OR GRANT NO.	9a. ORIGINATOR'S REPORT NUMBER(S)
Contract N00014-67-A-0112-0066	Technical Report 3
b. PROJECT NO.	SU-SEL-72-021
ARPA Order No. 1733; Program Code 2E20	9b. OTHER REPORT NO(S) (Any other numbers that may be assigned this report)
c.	
d.	

10. DISTRIBUTION STATEMENT

Approved for public release; distribution unlimited.

11. SUPPLEMENTARY NOTES	12. SPONSORING MILITARY ACTIVITY
Sponsored by ARPA and monitored by ONR (Code 418)	Office of Naval Research Field Projects Programs, Code 418 Arlington, Virginia 22217

13. ABSTRACT

Hydromagnetic waves associated with Pc 1 geomagnetic micropulsations travelling in the ionosphere should produce small ionospheric electron-density fluctuations. A search was made for such fluctuations using a ground-based HF sounding technique, but none were detected. This result is discussed in terms of the maximum fluctuation amplitude expected and the limitations on experimental sensitivity.

I

DD FORM 1 NOV 68 1473 (PAGE 1)

S/N 0101-807-6801

UNCLASSIFIED

Security Classification

14 KEY WORDS	LINK A		LINK B		LINK C	
	ROLE	WT	ROLE	WT	ROLE	WT
Micropulsations						
Geomagnetic micropulsations						
Hydromagnetic waves						
Electron density						
HF sounding						
Ionosphere						

II

SU-SEL-72-021

A SEARCH FOR IONOSPHERIC DISTURBANCES ASSOCIATED WITH Pc 1 MICROPULSATIONS

by

Bruce Dingle

March 1972

Technical Report No. 3

Sponsored by

National Science Foundation
(Grant GA-17486)

and

Defense Advanced Research Projects Agency
(ARPA Order No. 1733; Program Code No. 2E20)
through the Office of Naval Research
(Contract No. N00014-67-A-0112-0066)

Radioscience Laboratory
Stanford Electronics Laboratories
Stanford University Stanford, California

III

CONTENTS

CONTENTS (continued)

ILLUSTRATIONS

TABLES

ACKNOWLEDGEMENTS

This experiment was conceived and directed by Dr. A. C. Fraser-Smith. Professor O. G. Villard, Jr. was instrumental in its inception and provided many helpful suggestions throughout.

The National Science Foundation supported the experimental work under grant GA-17486, while the theoretical work and report preparation were sponsored by the Defense Advanced Research Projects Agency through the Office of Naval Research under contract N00014-67-A-0112-0066.

I. INTRODUCTION

A. PURPOSE

This report describes an experiment intended to detect possible electron-density perturbations in the ionosphere associated with small travelling fluctuations of the earth's magnetic field. The estimated size of the perturbations and the problems involved in their detection are discussed.

B. BACKGROUND

In 1722 George Graham, a London instrument maker, observed that a compass needle is never completely at rest but instead oscillates continually about its mean heading. It was thus discovered that the earth's magnetic field is in a continual state of flux. The nature of this variability has been the subject of considerable investigation for the ensuing two and one-half centuries.

Many observed magnetic fluctuations have a quasi-periodic structure. These form a group of disturbances called geomagnetic micropulsations, the "micro" prefix stemming from the fact that their amplitudes are very small in relation to the mean value of the earth's field. A further classification sorts these micropulsations into a number of subgroups based on their morphological properties. This report is concerned with particular properties of the Pc 1 micropulsations, a subgroup composed of regular magnetic-field oscillations having frequencies in the range 0.2 to 5 Hz. At middle latitudes these oscillations are primarily nighttime phenomena having amplitudes ranging from a few milligammas to hundreds of milligammas, and persisting from a few minutes to several hours. The classification of micropulsations and the units in which they are measured are discussed in more detail in Appendix A.

Pc 1 micropulsations apparently originate as plasma instabilities in the equatorial magnetosphere, from which region they travel down to the earth's surface along high-latitude magnetic field lines as

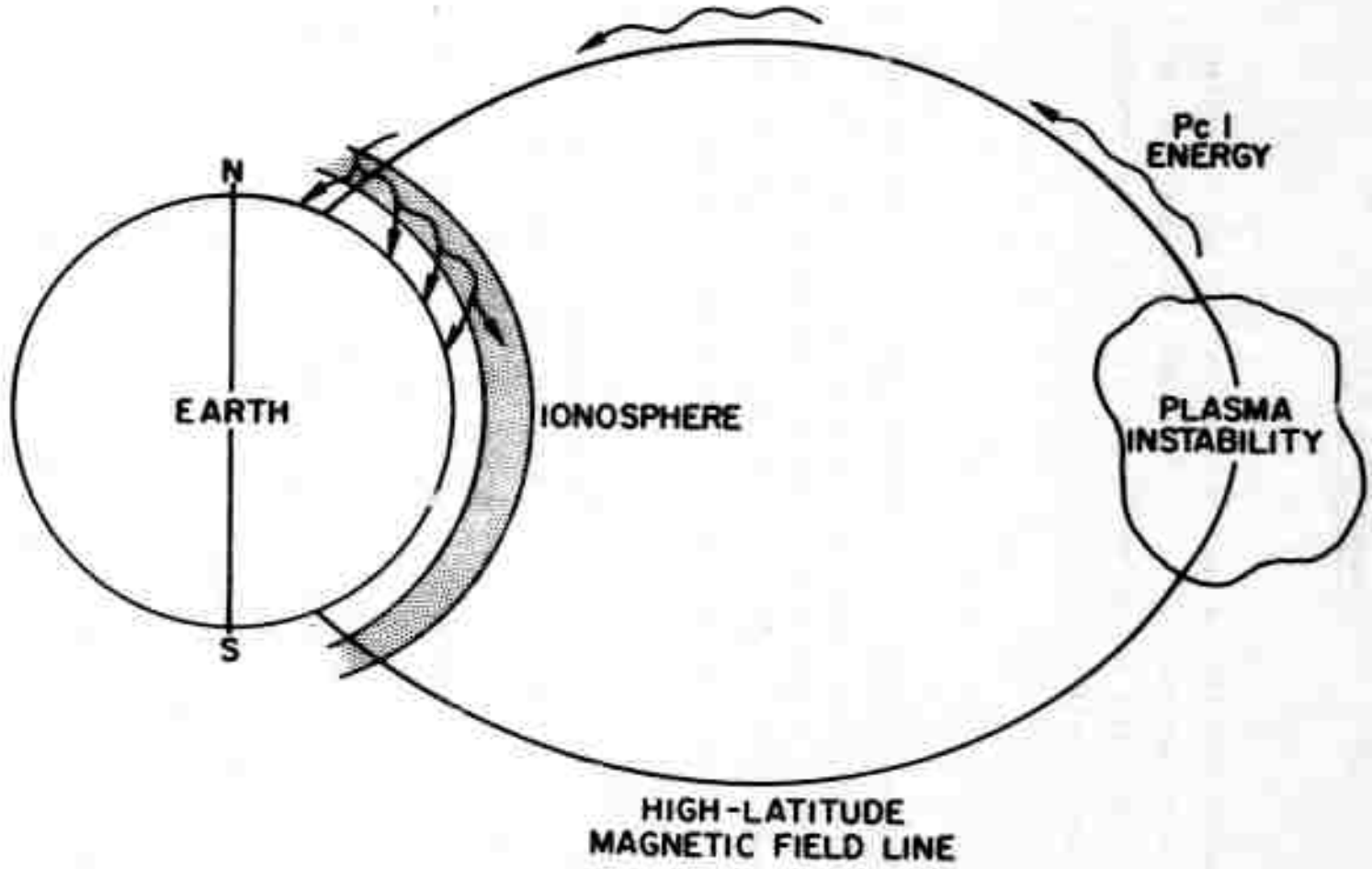

Figure 1. A schematic diagram of the propagation path of Pc 1 micropulsations from their point of origin in the magnetosphere to the surface of the earth.

hydromagnetic waves.* Figure 1 is a schematic representation of this situation. Given no other propagation mechanisms, it might be expected that the micropulsations would only be observed near the points where the disturbed magnetic field lines penetrate the earth's surface. However, Pc 1's are observed worldwide, although the strongest and most frequent occurrences are indeed at high latitudes.

Of particular interest is the observation that the occurrence of a Pc 1 micropulsation outburst at a middle-latitude location is often correlated with similar activity at high latitudes on the same geomagnetic meridian. In addition, the middle-latitude event is usually observed to be delayed in time with respect to the corresponding high-latitude event, as if the energy causing the disturbances had travelled with a measurable velocity from north to south (in the northern hemisphere). The propagation velocity which results from a consideration of the time and distance between the observations turns out to be approximately the group velocity of a hydromagnetic wave of Pc 1 frequency travelling in the ionosphere near the region of maximum electron density. Hence the theory has arisen that Pc 1 micropulsation energy travels from high to middle latitudes as a hydromagnetic wave and that a significant portion of the wave energy is confined to the ionosphere. This concept is also shown schematically in Figure 1.

A more detailed discussion of the theory describing the creation and propagation of micropulsations, as well as further information on their properties and classification, are given in Jacobs (1970). He reviews the whole micropulsation field and includes a good bibliography. In addition, a good account of the early history of geomagnetism can be found in Chapman and Bartels (1940).

C. METHOD OF OPERATION

A hydromagnetic wave with a frequency of about one Hertz travelling through a plasma with the attributes of the earth's ionosphere should induce in this plasma a periodic electron-density perturbation having

---

* Some of the terms introduced in this section (plasma, hydromagnetic wave, ionosphere and magnetosphere) are defined in Appendix B.

the same frequency (Fraser-Smith, 1969). If such a perturbation could be observed in the ionosphere while micropulsations were being observed on the ground, then support would be lent to the theory that the micropulsation energy flows from high to middle latitudes primarily in the ionosphere.

A high-frequency (HF) radio wave launched vertically from the ground will be reflected by the free electrons of the ionospheric plasma (provided that the wave frequency is not higher than the critical frequency) and will return to the vicinity of the transmitter. At the ground, the phase of the reflected wave will vary with respect to the phase of the transmitted wave if the electron density along the transmission path varies with time. In particular, a periodic electron-density perturbation induced by the passage of micropulsation energy should produce a periodic phase modulation of the reflected wave. Detection of periodic electron-density perturbations in the ionosphere is thus reduced to detection of phase modulation of a radio wave.

An experimental system designed to detect Pc 1 micropulsation energy in the ionosphere in the manner described above was set up by the Stanford University Radioscience Laboratory in mid-1970. A low-power HF wave was transmitted from a site near Pescadero, California, and was received on the university campus a few miles away after being reflected by the ionosphere. The theoretical and practical aspects of this project, as well as the experimental results, are discussed in the following pages.

II. MICROPULSATIONS AND THE IONOSPHERE

A. THE PREDICTION PROBLEM

Of fundamental concern is the size of the effect being studied. How great a fluctuation in the ionospheric electron concentration is to be expected, and how much influence will such a fluctuation have on a probing HF wave?

Starting with the theory of Pc 1 propagation outlined in Chapter I and making simplifying assumptions as necessary, we can proceed to make approximate calculations of the magnitudes in question. The investigation will be concerned with the middle-latitude nighttime ionosphere in the northern hemisphere, and the presence of Pc 1 micropulsation energy travelling southward will be assumed. The approach will be to use the simplest models that account for the relevant physical properties of this system.

In what follows, whenever the coordinate system needs to be related to the earth, the directions x, y, z refer to south, east and up respectively. The geomagnetic field is assumed to be oriented parallel to the z axis and thus to be vertical. Note that the discussion initially refers to a quite general plasma; parameters are then chosen so that this plasma models the physical earth-ionosphere system.

B. IONOSPHERIC ELECTRON-DENSITY PERTURBATION

For the purpose of estimating the size of the ionospheric electron-density perturbation we will examine the simplest plasma that will permit propagation of a hydromagnetic wave. Consider an unbounded, cold and collisionless plasma which in the unperturbed state is homogeneous and at rest. We require that this plasma be pervaded by a uniform magnetostatic field of strength B_o tesla, and then establish a cartesian coordinate system in the plasma so oriented that the z axis is parallel to the magnetostatic field. Then all of the possible modes of propagation of any monochromatic plane electromagnetic wave with its wave normal lying in the x-z plane are described by the equation

$$\begin{bmatrix} \epsilon_\perp - n^2\cos^2\theta & -i\epsilon_x & n^2\sin\theta\cos\theta \\ i\epsilon_x & \epsilon_\perp - n^2 & 0 \\ n^2\sin\theta\cos\theta & 0 & \epsilon_{||} - n^2\sin^2\theta \end{bmatrix} \begin{bmatrix} E_x \\ E_y \\ E_z \end{bmatrix} = 0 \quad . \tag{1}$$

Here n is the refractive index of the plasma and θ is the angle between the wave normal and the positive z-axis. The vector $\bar{E} = (E_x, E_y, E_z)$ represents the (time-varying) electric field of the electromagnetic wave and the ϵ's are components of the effective tensor permittivity of the plasma as given in Appendix C, where equation (1) is derived.

Physically we are interested in a hydromagnetic wave travelling horizontally in the mid-latitude ionosphere and therefore crossing lines of the earth's magnetostatic field at steep incidence. We will simulate this situation in our model by considering a wave moving along the positive x-axis. When (1) is solved with θ set equal to 90°, it can be shown (Clemmow and Dougherty, 1969) that there are two possible modes in which such a wave can propagate. However, in a plasma having an electron density approximating that of the ionospheric F region and at the low frequencies of interest in this study (that is, frequencies near 1 Hz), only one of these modes can propagate. For this mode

$$n^2 = \frac{\epsilon_\perp^2 - \epsilon_x^2}{\epsilon_\perp} \quad .$$

When this value of n^2 is inserted, (1) reduces to

$$E_x = i\,\frac{\epsilon_x}{\epsilon_\perp}\,E_y \text{ and } E_z = 0 \quad .$$

Invoking Maxwell's equation for the curl of $\bar{E}$, the components of the wave magnetic field $\bar{B}$ are discovered to be

$$B_z = \frac{n}{c}\,E_y \text{ and } B_x = B_y = 0 \quad ,$$

where c is the vacuum speed of light.

Since a wave frequency of 1 Hz is much less than the ion cyclotron frequency of our ionosphere-approximating plasma, the following approximations may be made as discussed in Appendix C:

$$\epsilon_\perp \approx \frac{c^2}{v_A^2} \text{ and } \epsilon_x \approx 0 \quad ,$$

where v_A is the Alfvén speed. The wave field components now reduce to

$$E_y = v_A B_z \text{ and } E_x = E_z = B_x = B_y = 0 \quad .$$

We now confine our attention to the electron motions controlled by these fields. Let N and ΔN be respectively the unperturbed electron number density and the perturbation thereof caused by the passage of our wave. Then from the charge conservation equation,

$$\frac{\Delta N}{N} \approx \frac{v_x}{v_A}$$

where v_x is the x component of electron velocity. From the Lorentz force equation

$$\frac{v_x}{v_A} \approx \frac{B_z}{B_o} \quad .$$

These last two equations combine to give

$$\frac{\Delta N}{N} = \frac{B_z}{B_o} \quad . \qquad (2)$$

That is, the fractional electron-density perturbation is equal to the ratio of the amplitude of the wave magnetic field component parallel to the magnetostatic field to the amplitude of the magnetostatic field itself. This equation is the central relationship for this experiment since it enables calculation of the electron-density perturbation

when the wave magnetic field strength is known, and vice versa.

C. FIELD VARIATION WITH ALTITUDE

The plasma model discussed in Section B is unbounded and uniform - that is, it exists in some imaginary space and has no connection with the earth. This is a reasonable model for the ionosphere but cannot, however, give much idea of what happens at the earth's surface. And a connection with the earth must be made since the only method we have at present of estimating the size of micropulsation wave fields in the ionosphere is by making measurements at the ground.

There are two principal objections to the model used in Section B. The first is that the actual electron density in the atmosphere is not uniform with altitude, but varies in a manner similar to that shown in Figure 10 of Appendix B. A height-dependent electron density must be introduced if we are to model waves at the ground and in the ionosphere simultaneously. Secondly, there is actually a sharp boundary at the surface of the earth since the earth is a good electrical conductor at frequencies near 1 Hz. Our model should be similarly bounded if effects near the existing real boundary are to be approximated.

A convenient model which meets the requirements laid down in the previous paragraph is one used by Greifinger and Greifinger (1968). A plot of the electron-density variation with height for this model is shown in Figure 2. The coordinate system is related to the earth in the manner discussed in Section A. The earth itself is taken to be flat and perfectly conducting, providing a sharp bound at $z = 0$. Hence the model is semi-infinite in the z direction but is still unbounded in the x and y directions. The dimensions of the model are consistent with nighttime, sunspot-minimum conditions.

The Greifingers develop equations in their article which describe the fields associated with a 1-Hz hydromagnetic wave travelling horizontally in this model. The magnetic field components of such a wave moving southward are plotted in Figure 2. Now B_z in the ionosphere (B_{zm}) is proportional to the fractional electron-density perturbation there to the extent that equation (2) can still be considered valid; moreover, B_x at the ground (B_{xo}) can be measured. Since the ratio of these two

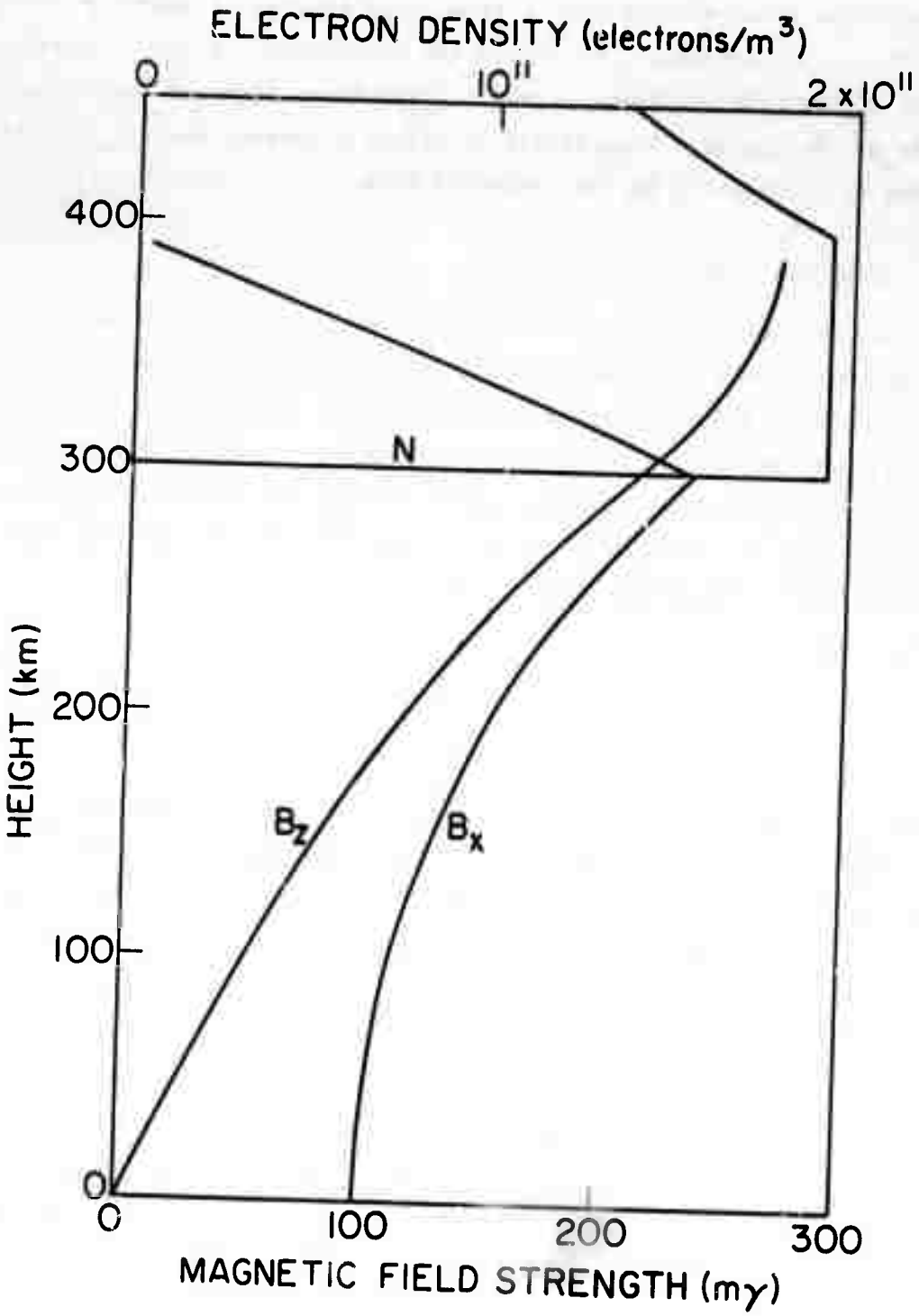

Figure 2. The electron-density profile of the model ionosphere discussed in the text, and the height variation of the two components of the magnetic wave field of a 1-Hz micropulsation travelling in this ionosphere. B_x at the ground is arbitrarily chosen to be 100 mγ. The ratio of B_z in the ionosphere to B_x at the ground is roughly 2·5.

quantities is a constant (for a fixed wave frequency), knowing its value enables us to estimate the size of the wave fields in the ionosphere, and thus of the electron-density perturbation there, given a measurement made on the ground. Examination of Figure 2 reveals that B_{zm}/B_{xo} has a value of roughly 2.5 for our model at 1 Hz.

D. DETECTING THE DISTURBANCE

Given that there is a certain electron-density disturbance in the ionosphere, how is the phase of a probing HF signal affected? To answer this question let us again consider the model discussed in Section C, except that we now set $B_o = 0$ since the presence of the magnetostatic field does not affect the essence of the HF propagation now under discussion.

If N(z) is the electron-density distribution with height, then the square of the refractive index is given by

$$n^2 = 1 - \frac{f_p^2}{f^2} = 1 - AN \quad .$$

Here f_p ($= 9N^{1/2}$ in mks units) is the electron plasma frequency, f is the HF wave frequency, and $A = 81/f^2$ is a convenient parameter (see Budden, 1961). Using this equation we can solve for the refractive index perturbation Δn caused by an electron density change ΔN:

$$\Delta n = -n + (n^2 - A\Delta N)^{1/2} \quad . \qquad (3)$$

The next step is to examine the phase path of a vertically-incident radio wave. If z_r is the height at which the wave is reflected, then the phase path (see Budden) is

$$P = 2 \int_0^{z_r} n \, dz \quad .$$

For refractive index perturbation Δn, and assuming that the resulting Δz_r is small, the phase-path change is

$$\Delta P \approx 2 \int_0^{z_r} \Delta n \, dz \quad . \tag{4}$$

When the phase-path change and the free-space HF wavelength are known, then the number of degrees of phase change of the reflected radio wave is easily calculated.

E. A NUMERICAL ESTIMATE

To get a quick numerical estimate of the phase change that might result from the passage of a typical Pc 1 micropulsation in the ionosphere, let us evaluate equation (4) using the model of Figure 2. Choose $z_r = 400$ km and $f^2 = \frac{4}{3} f_p^2$. Assuming that equation (2) holds everywhere in the ionized region, and using the result of Section C that $B_{zm}/B_{xo} \approx 2.5$ at 1 Hz,

$$\frac{\Delta N}{N} \approx \frac{2.5 \times 100 \text{ m}\gamma}{0.5 \text{ gauss}} = 5 \times 10^{-6}$$

for a measured field on the ground of 100 mγ peak-to-peak and a static field of 0.5 gauss. We will take $\Delta N/N$ to be constant in the region of interest. Substituting into (3) and (4),

$$\Delta P = -7.5 \times 10^{-6} \int_{300 \text{ km}}^{400 \text{ km}} dz = -0.75 \text{ m} \quad .$$

For an HF wavelength of 72 meters, this represents $0.75 \times 360°/72 \approx 3.8°$ of phase swing. In other words, we might reasonably expect that the phase of the probing signal would vary over a range of something like a few degrees in a typical situation.

III. NOISE

A. NOISE SOURCES

The problem of detecting a small phase modulation of an ionospherically-reflected wave is complicated by the presence of a number of contaminating signals. These signals can be roughly classified in the following manner:

(i) background noise,

(ii) phase noise imposed by the ionosphere,

(iii) spurious reflections of the transmitted signal.

Interference from other transmitters is neglected since the receiving system is narrowband and unwanted carriers are easily avoided. Noise introduced by the detection system is generally negligible compared to the external noise and is not discussed here.

B. BACKGROUND NOISE

The background noise is assumed, not unreasonably, to be Gaussian white noise. This white noise is filtered by the bandpass characteristic of the receiver and becomes narrowband noise which can be represented by the expression $n(t)=a_n \cos(\omega t+\varphi_n)$ where a_n and φ_n are random processes (Carlson, 1968).

The noise adds to the desired signal $x(t) = a \cos(\omega t + \varphi)$ to yield

$$\begin{aligned} s(t) &= x(t) + n(t) \\ &= a \cos(\omega t + \varphi) + a_n \cos(\omega t + \varphi_n) \\ &= M \cos(\omega t + \Psi) \end{aligned}$$

where expressions for M and Ψ can be found by algebraic manipulation. When the assumption is made that $a_n \ll a$ most of the time, as is usually the case in practice, then Ψ is given by

$$\Psi = \varphi - \frac{a_n}{a} \sin(\varphi - \varphi_n) \quad .$$

The power spectrum of the second term in this expression is just the power spectrum of the original noise but diminished by the factor $1/a^2$ (Carlson, 1968). Hence the additive noise is transformed directly to additive Gaussian narrowband phase noise, but with the noise power reduced according to the strength of the transmitted carrier. For the experiment under consideration in this report, the carrier and noise levels were generally such that background noise was not a limiting factor.

C. IONOSPHERIC PHASE NOISE

The electron density and thus the refractive index along the path of a radio wave travelling through the ionosphere are continually and randomly varying with time. This variation modulates the phase of our received wave and hence is a noise source. The effect is probably quite small, however, especially since the expression for the received phase involves an integral over the path. In any event, such noise cannot be easily separated from that due to spurious reflections and will be neglected from here on.

D. SPURIOUS REFLECTIONS

Energy radiated from a simple horizontal dipole antenna can reach a receiving antenna some short distance away by a multitude of paths. Assuming that the groundwave is blocked in some way, all the signal paths involve ionospheric reflection. The number of paths and their propagation characteristics depend on the roughness and turbulence of the ionosphere at any particular time.

The simplest case that one can expect to encounter occurs at times when the ionosphere is effectively a smooth reflector of radio waves. In such a situation the signal arriving at the receiver is the combination of several components since the original wave has divided into ordinary and extraordinary components and because some of the wave energy has made multiple ground-ionosphere-ground hops before being received. The ordinary and extraordinary components reflect at different heights but have comparable amplitudes and, assuming the presence of a periodic

electron-density perturbation, comparable levels of phase modulation. Each successive hop, however, has a greater level of phase modulation than its predecessor because it has passed through the modulating region more often, but is lower in amplitude because it has suffered more ionospheric attenuation and has travelled farther. Each component is in general reflected from a different point in the ionosphere, but these points are within a few tens of kilometers of each other for near-vertical incidence. Since we are interested in ionospheric disturbances with large horizontal scale size (on the order of 1000 km), we can assume that the modulation imposed on each component is approximately in phase with the modulation imposed on all the other components. However, the carrier phase of each component is completely random with respect to the carrier phases of the other components. In addition, the carrier frequency of each component has a distinct doppler shift since each reflection point has in general a distinct effective vertical velocity.

Some computer simulations were made of the smooth-ionosphere situation and the results of these indicate that doppler shifts of the component carrier frequencies provide most of the noise in the phase spectrum of the received signal. The net phase modulation level at the receiving antenna is not very different from the level that would be expected if there were only one path between transmitter and receiver, but the phase spectrum fills with noise as doppler shifts are introduced. However, for moderate doppler shifts consistent with reasonably settled ionospheric conditions, phase modulation levels of a few degrees of phase swing can be readily detected above the noise. Of course when the ionosphere becomes rough and turbulent, then the number of signal components and the size of the doppler offsets increase and more phase noise is produced, eventually obscuring the phase modulation. In practice, there is some "normal" level of ionospheric disturbance which determines a minimum level of phase modulation that can be detected; this threshold is determined by experimental measurement.

IV. THE APPARATUS

A. EXPERIMENTAL ARRANGEMENT

The experiment was implemented using a simple continuous-wave (CW) transmitter in conjunction with a narrowband receiver and phase demodulator. The transmitter site was established at a location on the Pacific coast of California about 28 km from the receiver site on the Stanford University campus. The geographical layout is illustrated in Figure 3. The range of hills running between the two sites eliminated groundwave propagation. Hence the main signal path between the two sites was the one-hop ionospheric route. This was essentially a vertical path due to the relatively small separation between transmitter and receiver.

The transmitter radiated approximately 100 watts at about 4 MHz from a horizontal half-wave dipole antenna. A similar antenna was used at the receiver site. Call-letter keying and a calibration modulation were applied to the transmitted signal as described in Section C of this chapter.

The receiving system is outlined in Figure 4. The 4-MHz input is down-converted to 100 Hz with a bandwidth of 10 Hz. From this point the signal is demodulated, recorded, and eventually processed as indicated by the succeeding blocks in Figure 4.

Supplementing this primary equipment, a geomagnetic micropulsation recording station and a vertical ionosonde were in operation on the Stanford campus. The micropulsation station continuously recorded the time-varying horizontal north-south (geographic) component of the earth's magnetic field. The ionosonde provided vertical ionograms several times each hour of the day.

B. THE DEMODULATOR

The demodulator is a phase-locked loop as diagrammed in Figure 5. The voltage controlled oscillator (VCO) operates nominally at the same frequency and phase as the input signal. It follows slow input-phase variations and maintains the phase-detector outputs at zero. However,

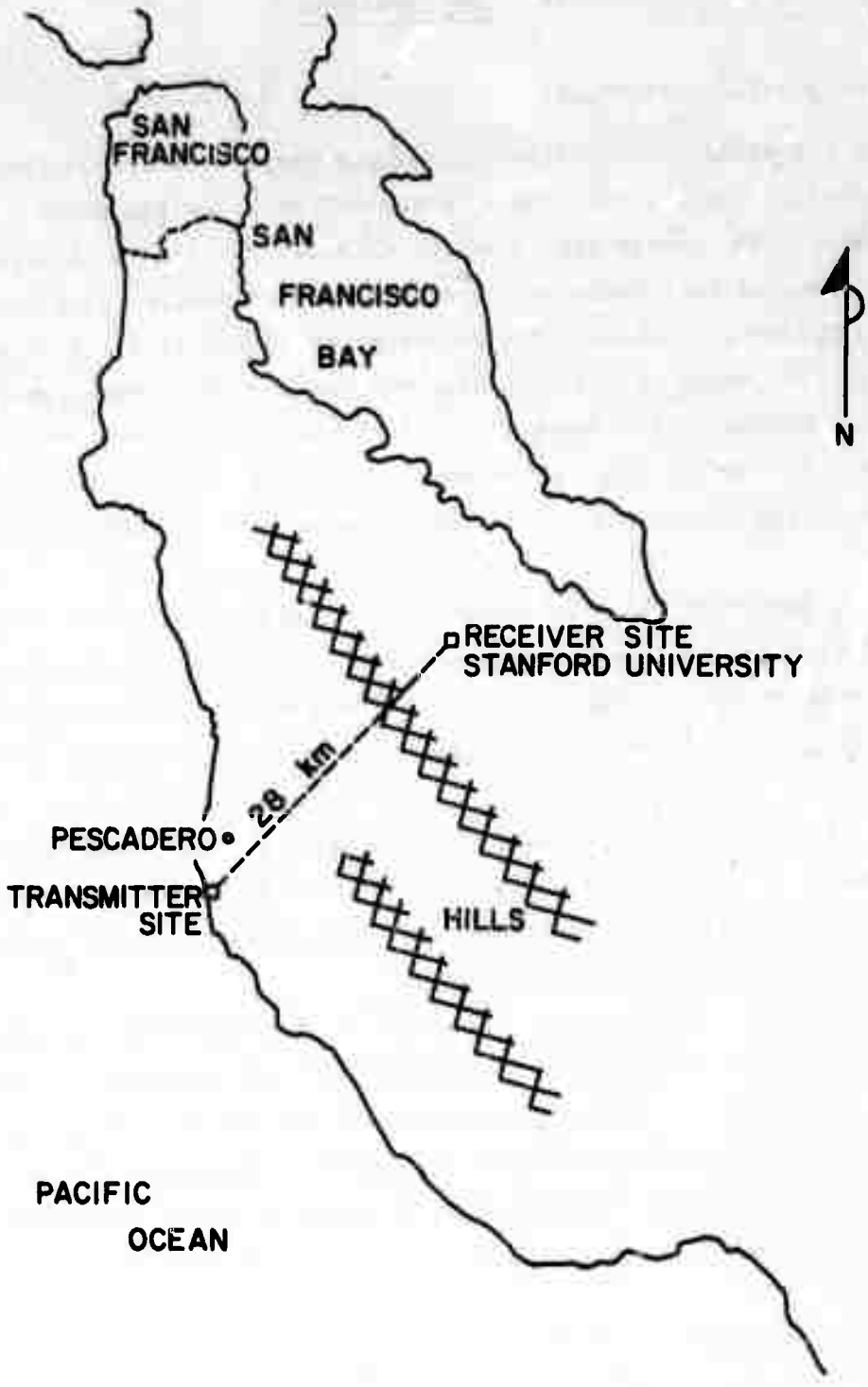

Figure 3. Geographical layout of the experimental apparatus.

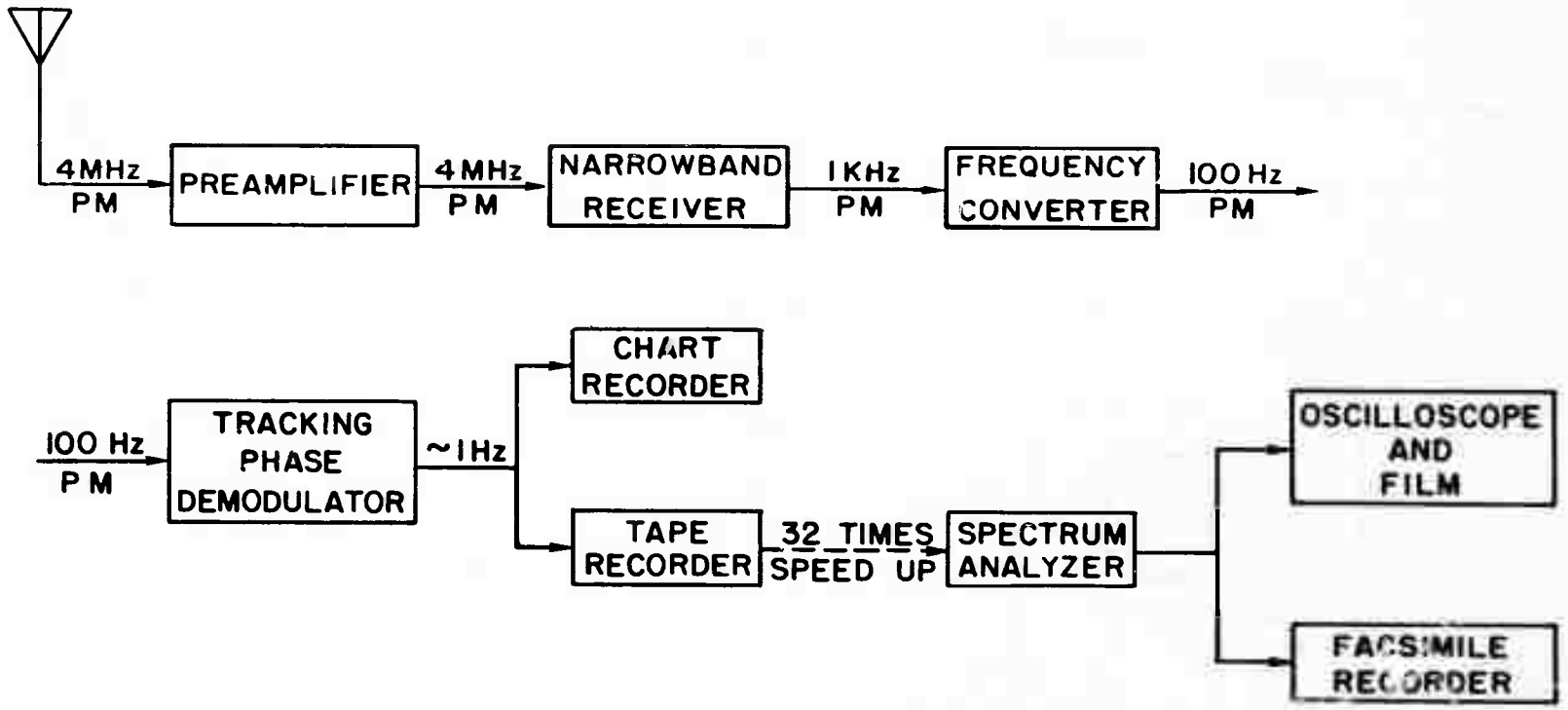

Figure 4. Block diagram of the receiving system.

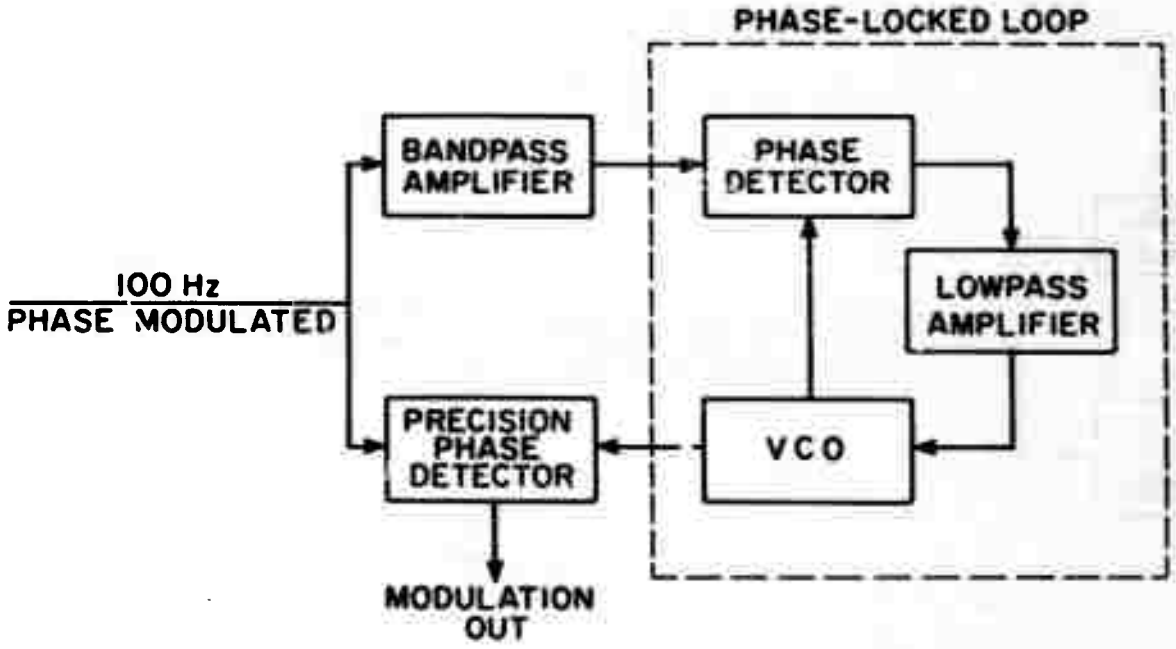

Figure 5. Block diagram of the demodulator.

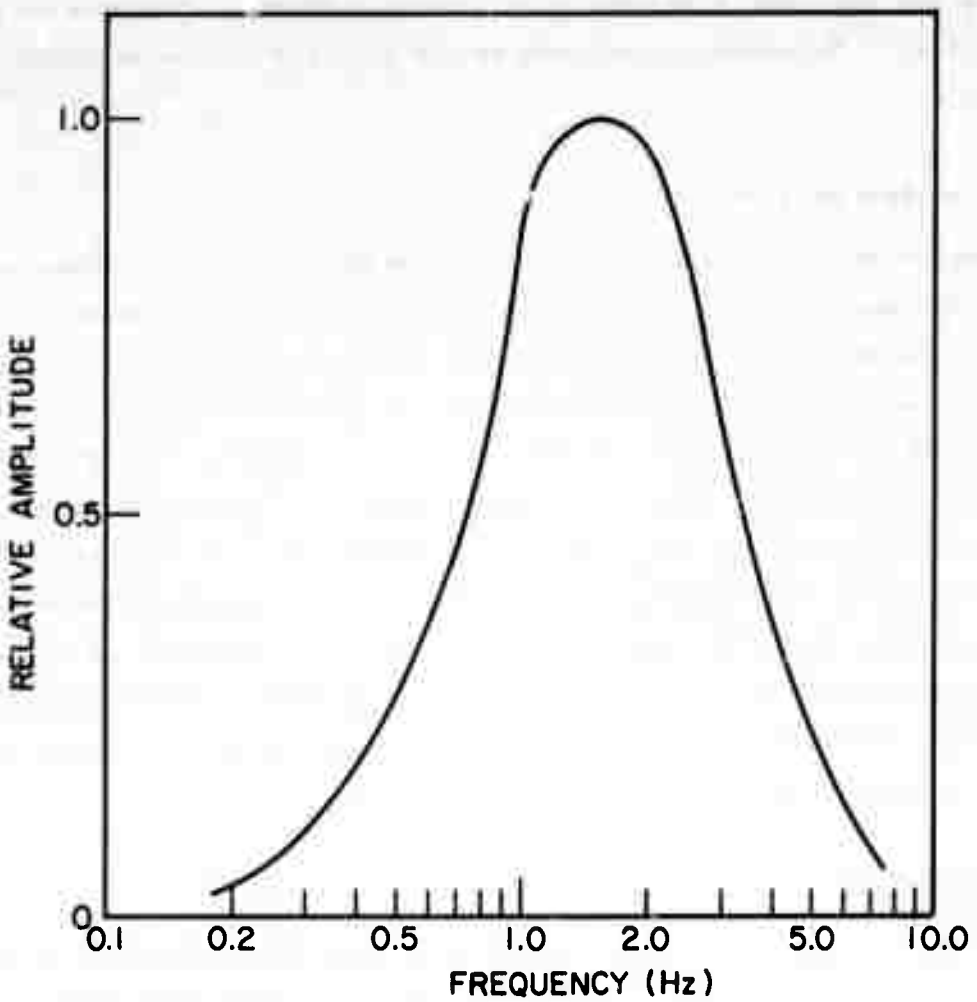

Figure 6. Frequency response of the receiving system to phase modulation.

due to the effect of the lowpass amplifier, the VCO cannot follow rapid input-phase variations. Hence rapid variations will appear as output of both phase detectors. In other words, the loop itself has a highpass response to phase modulation. However, the narrow bandwidths of the preceding stages of the receiver limit the high-frequency response of the system and the overall effect is to produce a bandpass response to phase modulation. The measured response of the receiver system is shown in Figure 6.

C. CALIBRATION SIGNAL

Noise is a major component of the demodulator output. There are contributions from both the ionosphere and the receiver. Since the signals being sought are very small, it is necessary to know at any time what the smallest detectable signal is. For this reason a calibrated phase modulation is applied to the transmitted signal. Its intensity is stepped over a range of values in order that the minimum detectable signal at any point in time can be determined simply by examining the output record. The standard calibration format is given in Table 1. The receiving system is capable of resolving less than 0.5° of phase swing, but this level of performance is not attainable under actual operating conditions because of the presence of ionospheric noise (as described in Chapter III).

D. RECORDING AND REDUCTION

The demodulator output is recorded on magnetic tape and on a strip chart. The chart records, examples of which are shown in Figure 7, give a real-time determination of propagation conditions and general system operation. The magnetic tape provides the main data record.

It is often very difficult to understand amplitude-time records because of the complexity of the signals and the presence of noise. Hence the data stored on magnetic tape is converted to frequency-time form for easier study. This is accomplished using an analog spectrum analyzer and a tape playback speed thirty-two times greater than the recording speed. The increased speed keeps the amount of time required

TABLE 1

Modulation and Keying Schedule

Minutes after Hour or Half Hour	Modulation Level (peak-to-peak phase swing)
0	call-letter keying
0.0 - 1.5	carrier off
1.5 - 3.0	0°
3.0 - 7.5	32°
7.5 - 12.0	16°
12.0 - 16.5	8°
16.5 - 21.0	4°
21.0 - 25.5	2°
25.5 - 28.5	0°
28.5 - 30.0	carrier off
30	call-letter keying

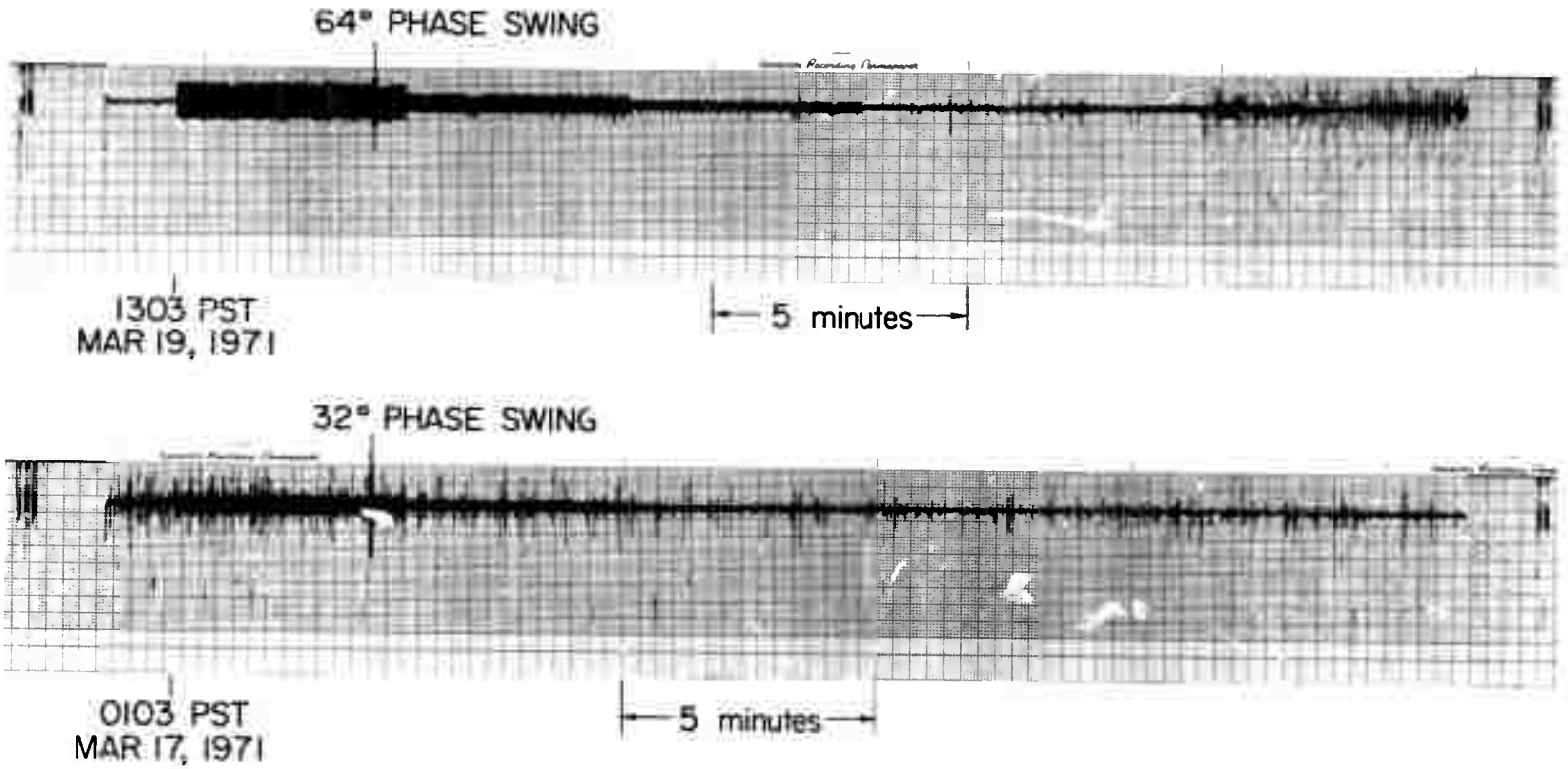

Figure 7. Sample chart records. Both records show phase of the received HF signal versus time. The lower record was made during typical nighttime conditions. The minimum detectable phase swing at that time (as observed by spectral analysis) was about 4°; that is, 4° peak-to-peak phase modulation amplitude. The upper chart is a daytime record shown for comparison; the calibration levels are twice those used at night. There is very little noise and the lowest calibration level (4° in this case) was well above the detection limit on the associated spectral record.

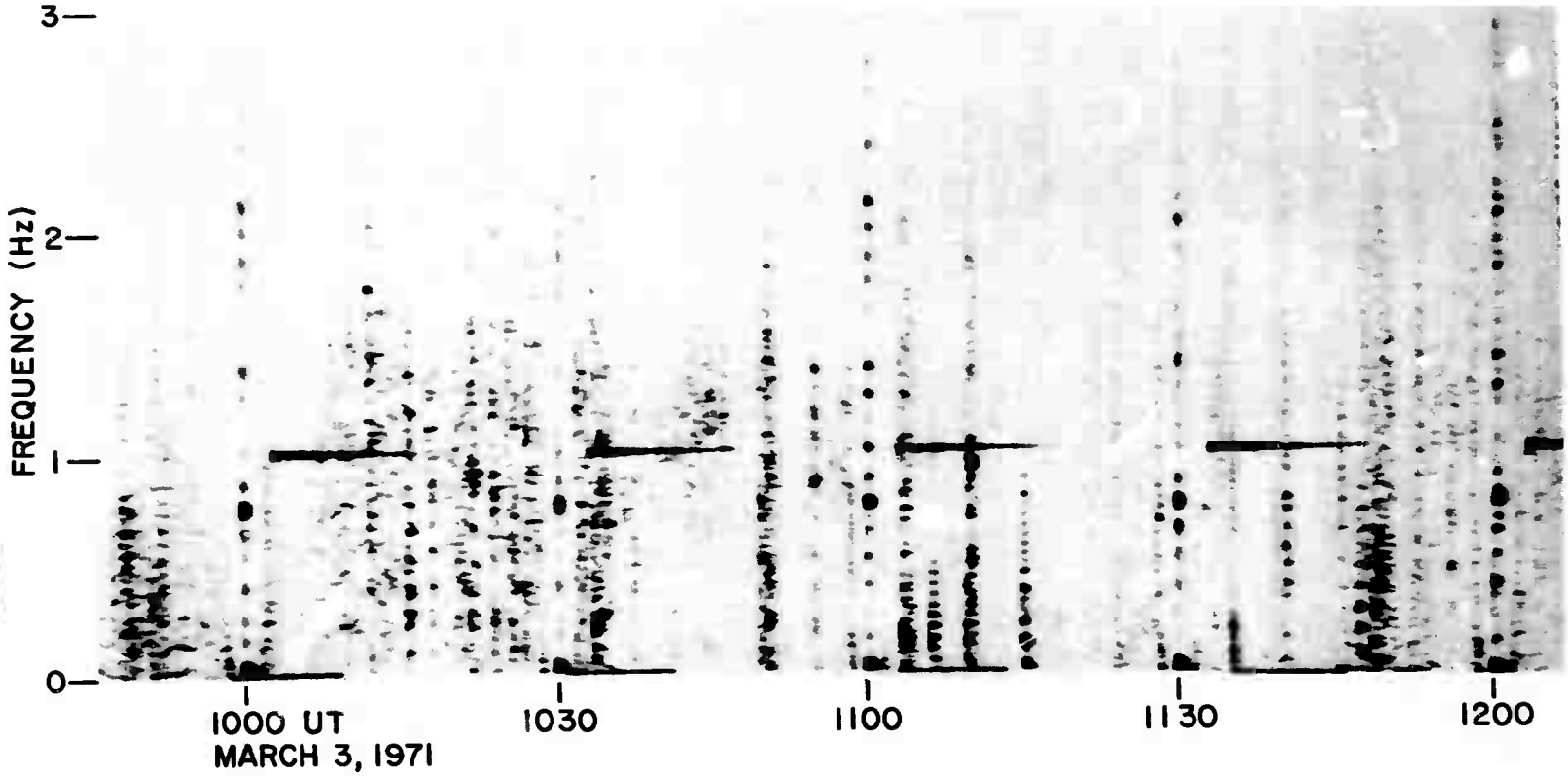

Figure 8. A facsimile-recorded phase spectrum. The minimum detectable phase modulation level in this instance, as determined by the duration of the 1-Hz calibration signal, is about 4° of phase swing. Although a Pc 1 micropulsation event was in progress at this time, there is no evidence of its presence on this record.

required for playback at a practical level (about eleven minutes for six hours of data) and provides a signal frequency more suited to the spectrum analyzer.

The analyzer output is recorded either photographically or by a facsimile process. In each case the record shows a plot of frequency versus time of day, with signal strength indicated by relative darkening of the film negative or facsimile paper. The film record is produced by pulling film across the face of an oscilloscope whose x and z axes are driven respectively by the frequency and amplitude outputs of the analyzer. The facsimile record is formed on chemically-treated paper by a special recorder. An advantage of the facsimile process is that it provides immediately-visible output which allows for the expeditious setting of gains and speeds, whereas film must first be developed before any feedback can be applied. An example of the facsimile output is shown in Figure 8.

V. RESULTS

A. EXPERIMENTAL PROCEDURE

The nominal procedure was to record phase variations of the HF signal for a six-hour period each night (usually from 2300 to 0500 PST). This was done intermittently over the interval from June 18, 1970 to December 31, 1970, and essentially without interruption from January 1, 1971 to June 25, 1971. Equipment problems were responsible for most nights missed. The six-hour recording time was dictated by properties of the tape recorder, but proved long enough to provide coverage of most Pc 1 micropulsation events.

Any time that the micropulsation records showed that a Pc 1 event had occurred on the ground, the phase records were searched for evidence of coincident fluctuations. The ionograms for such times were also consulted to determine the proximity of the operating frequency to the ionospheric critical frequency.

B. Pc 1 MICROPULSATION OCCURRENCES

Over the year that the experiment was in operation, Pc 1 micropulsation activity occurred (at the ground) on an average of 5.5 nights per month. This activity is plotted on a monthly basis in Figure 9. A noticeable feature of the plot is the fall-winter minimum and spring-summer maximum of occurrences.

C. EXPERIMENTAL RESULTS

During the course of the experiment there were only 9 nights on which reasonably-sized micropulsations (50 mγ or greater peak-to-peak amplitude) occurred while the phase-measuring equipment was operating properly. No coincident phase-path fluctuations could be detected at any of these times.

Some of these events, including the largest ones, are listed in Table 2 along with values of relevant parameters. The probe frequency in all cases was about 4 MHz. The detection ratio used in Table 2 is

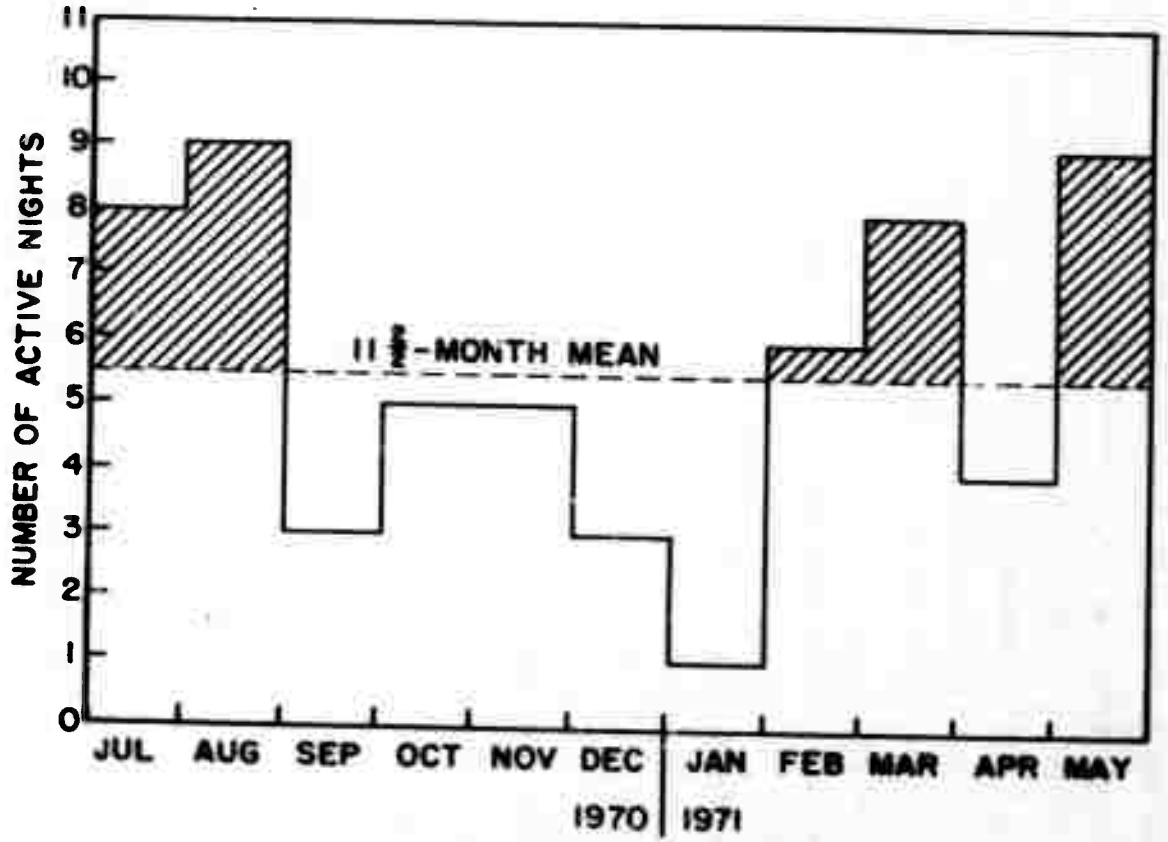

Figure 9. Occurrences of Pc 1 micropulsations at Stanford in 1970/71. The micropulsation recorder has a detection threshold of about 1 mγ. The mean monthly activity indicated by the dashed line includes data from the last two weeks of June, 1970 and the first two weeks of June, 1971--hence the label $11\frac{2}{2}$.

Table 2

Some Experimental Numbers

Date	Maximum Micropulsation Amplitude* (mγ peak-to-peak)	Minimum Detectable Modulation Level** (peak-to-peak phase swing)	Detection Ratio† (mγ/degree)	Penetration Frequency†† (MHz)
7 Aug 70	160	4°	40	4.8
14 Aug 70	200	4°	50	4.8
3 Mar 71	60	4°	15	4.3
17 Mar 71	70	8°	9	4.4
13 May 71	200	4°	50	5.0

* Data from Stanford micropulsation recording station.

** As observed on the corresponding phase spectrum.

† The ratio of column 2 to column 3, a measure of detection likelihood.

†† Average penetration frequency for the ordinary wave.

the ratio of the measured micropulsation amplitude to the minimum detectable phase-modulation level, and is a measure of the likelihood of observing phase-path fluctuations. Larger micropulsations or a lower detection threshold give higher values for this ratio.

In Chapter II the ratio B_{zm}/B_{xo} was estimated to be about 2.5 for 1-Hz micropulsations. Noting that the largest micropulsations observed had a peak-to-peak amplitude on the ground (B_{xo}) of 200 mγ, we can estimate that the fractional electron-density perturbation in the ionosphere must have been less than about 10^{-5} (taking $\Delta N/N=B_z/B_o$ and B_o = 0.5 gauss).

Table 2 demonstrates that the normal noise level corresponds to a minimum detectable phase swing of about 4°. Since the background noise level was low enough to be neglected, this noise presumably results from the effects of spurious reflections as was discussed in Chapter III.

D. DISCUSSION

The phase swing estimated for a typical micropulsation in Section E of Chapter II is of the same order of magnitude as the minimum detectable phase swing measured during the experiment. Although this leads to the expectation that the largest micropulsations might have produced an observable disturbance, it is not surprising, in light of the various approximations made in the preceding pages, that no such disturbances were indeed detected.

The models used in Chapter II neglect the inclination of the magnetostatic field and do not provide a very realistic N(z) profile. The assumption is made that equation (2) is valid at all heights, and only 1-Hz micropulsations are considered. The effect of the bandpass characteristic of the phase-locked loop is ignored, as is the integration time of the spectrum analyzer. All of these matters, and probably others as well, would have to be taken into consideration if a complete description of the processes involved in this experiment were to be given.*

*Much of this work has since been done by the author, but is not included here because it does not materially affect the results of this study.

The failure of the experiment to detect micropulsation disturbances reduces to the statement that the signal level must have been less than the detection threshold of the receiving system. The sensitivity of the equipment might be improved somewhat by such measures as using polarized and/or directive antennas to cut down on the spurious reflections received, or by improving the time- and frequency-response characteristics of the detection and data-reduction systems. However, assuming that little improvement can be made in the detection scheme, the best hope of achieving some positive results might be to relocate the experiment at a more northerly latitude where the amplitude of the micropulsations can be expected to be larger.

VI. CONCLUSIONS

Based on the approximate calculations made in Chapter II, and using the amplitude of the largest micropulsations observed on the ground, it can be estimated that the fractional electron-density perturbation produced in the ionosphere by travelling Pc 1 micropulsations is normally less than about 10 parts per million for geomagnetic latitudes lower than 45°.

In addition, the experimental detection scheme described in this report is limited, probably by the effect of spurious reflections, to a minimum detectable phase modulation level of about 4° of phase swing at night.

Working within the constraints of an upper bound on the electron-density perturbation and a minimum detectable phase change, the experiment was unable to detect any ionospheric disturbances associated with Pc 1 micropulsations.

APPENDICES

Preceding page blank

APPENDIX A

MICROPULSATION CLASSIFICATION AND UNITS

1. CLASSIFICATION

Based on experimental findings, geomagnetic micropulsations are divided into two main classes - those of a regular and mainly continuous character, and those with an irregular pattern. The first class covers the whole range of micropulsations with periods from about 0.2 to 600 seconds, and is divided into subgroups based on physical and morphological properties. Table 3 shows the classification and notation for these continous micropulsations.

Table 3

Continuous Micropulsations

Notation	Period Range (seconds)
Pc 1	0.2 - 5
Pc 2	5 - 10
Pc 3	10 - 45
Pc 4	45 - 150
Pc 5	150 - 600

The second main class of micropulsations is characterized by their irregular form, their close connection with disturbances of the geomagnetic field, and their correlation with various upper atmospheric phenomena. For this class there are two subgroups as shown in Table 4.

Table 4

Irregular Micropulsations

Notation	Period Range (seconds)
Pi 1	1 - 40
Pi 2	40 - 150

This description is taken from Jacobs (1970) where further details may be found.

2. UNITS

The earliest workers in the field of magnetism envisioned the magnetic field in terms of lines of force emanating from magnetic poles, where a pole was considered to be the magnetic equivalent of an electric point charge. Although magnetic poles have never been found to exist as independent entities, the concept of lines of force remains useful, and in fact the magnetic field strength B is conveniently described in terms of such lines. (The force that we are talking about here is that which would be exerted on a small, positive magnetic "charge" placed in the field.) At any point, B is directed along the force lines and is proportional in magnitude to the line density (that is, the number of lines passing through unit cross-sectional area). Note that B is historically called the magnetic induction, but is termed the magnetic field strength in this report since this is felt to be a more descriptive name.

The unit of B in the mks system is the tesla (or weber $/m^2$). For convenience, and following historical precedent, smaller units are usually employed, namely the gauss, the gamma, and the milligamma. Table 5 shows the relationships among these units.

Table 5

Units of Magnetic Field Strength

1 gauss (G)	$= 10^{-4}$ weber/m^2	=	100 microteslas
1 gamma (γ)	$= 10^{-5}$ gauss	=	1 nanotesla
1 milligamma (mγ)	$= 10^{-8}$ gauss	=	1 picotesla

APPENDIX B

DEFINITIONS

The following information is taken in large measure, and often almost verbatim, from Clemmow and Dougherty (1969), Rishbeth and Garriott (1969), and Utlaut and Cohen (1971).

1. PLASMA

A plasma is any assemblage of particles, some or all of which are charged, that can from the macroscopic view be regarded as a gas which in its equilibrium state is everywhere locally neutral. The fact that individual particles of the gas are charged, and therefore generate and interact with electromagnetic fields, gives rise to many distinctive phenomena.

The plasma frequency is the frequency of natural oscillation associated with the electrostatic restoring force arising from a small displacement of charge in a plasma. For plasmas in a magnetic field, it is often necessary to consider the gyro frequency (or cyclotron frequency); this is the frequency at which a charged particle moving at right angles to the field is forced to gyrate about the field lines.

When relative bulk motion of two plasmas is considered, the possibility of plasma instability arises. That is, electromagnetic waves can be generated or amplified in one of the plasmas by the process of extracting energy from the relatively-moving particles of the other plasma.

2. HYDROMAGNETIC WAVE

Low-frequency electromagnetic waves (that is, waves with frequencies much less than the ion gyro frequency) travelling through a plasma in a magnetostatic field have the property that, considering the associated motion of the charged particles, the velocity component perpendicular to the magnetostatic field is approximately the same for the electrons as for the ions. In its motion across the magnetostatic field, the plasma therefore moves as a whole. Furthermore, these waves travel at a speed which depends only on the mass density of the plasma and the strength of the magnetostatic field; this is the Alfvén speed.

Such waves are variously called hydromagnetic, magnetohydrodynamic (mhd), or Alfvén waves.

3. IONOSPHERE

The ionosphere is that region of the earth's atmosphere where ions and electrons are present in sufficient quantities to affect the propagation of radio waves. This region begins at an altitude of about 50 km and extends upward as shown by plots of electron concentration versus altitude such as the one given in Figure 10. The shape of these profiles varies diurnally, seasonally, with sunspot number, and with latitude and longitude. The profile peak usually occurs between 200 and 400 km; the portion of the ionosphere in the vicinity of the peak is commonly termed the F region or layer. In the F region the peak densities (number densities or concentrations) of ions (predominantly O^+ ions) and electrons are each about 10^{12} particles per cubic meter. The neutral particle density is about 10^{15} per cubic meter, implying only 0.1 percent or less ionization in this region. At about 1500 km, however, the ion and neutral-particle densities become roughly comparable, and this is a convenient point to label as the upper boundary of the ionosphere.

The free electrons, rather than the ions, interact more strongly with radio waves since they are much less massive, and it is the electron plasma frequency of the ionosphere which determines the level at which impinging radio waves are reflected. The maximum plasma frequency (which occurs at the electron density peak) is called the critical or penetration frequency of the ionosphere since vertically-incident waves of higher frequency will not be reflected but will pass through the ionosphere. The critical frequency typically lies between 3 and 6 MHz at night, and between 6 and 12 MHz during the day.

4. MAGNETOSPHERE

The magnetosphere is that region of the earth's atmosphere where the particle dynamics are primarily controlled by the geomagnetic field. Although the movement of ionization is geomagnetically controlled at all heights above 150 km (or even less), it is convenient to set the lower boundary of the magnetosphere at about 1500 km where the neutral particle density becomes predominant over the ion density. The magnetic field,

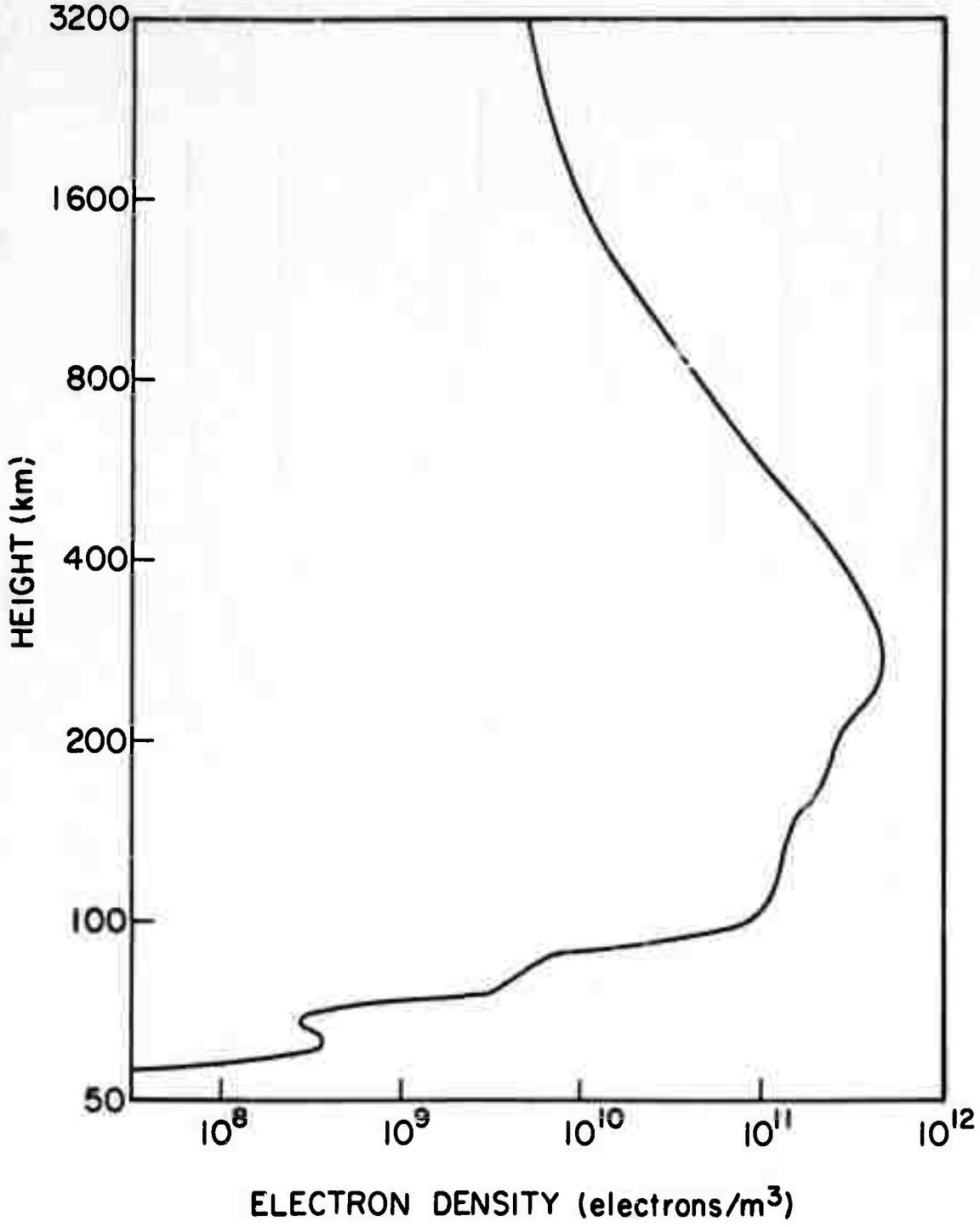

Figure 10. A typical daytime midlatitude electron-density profile.

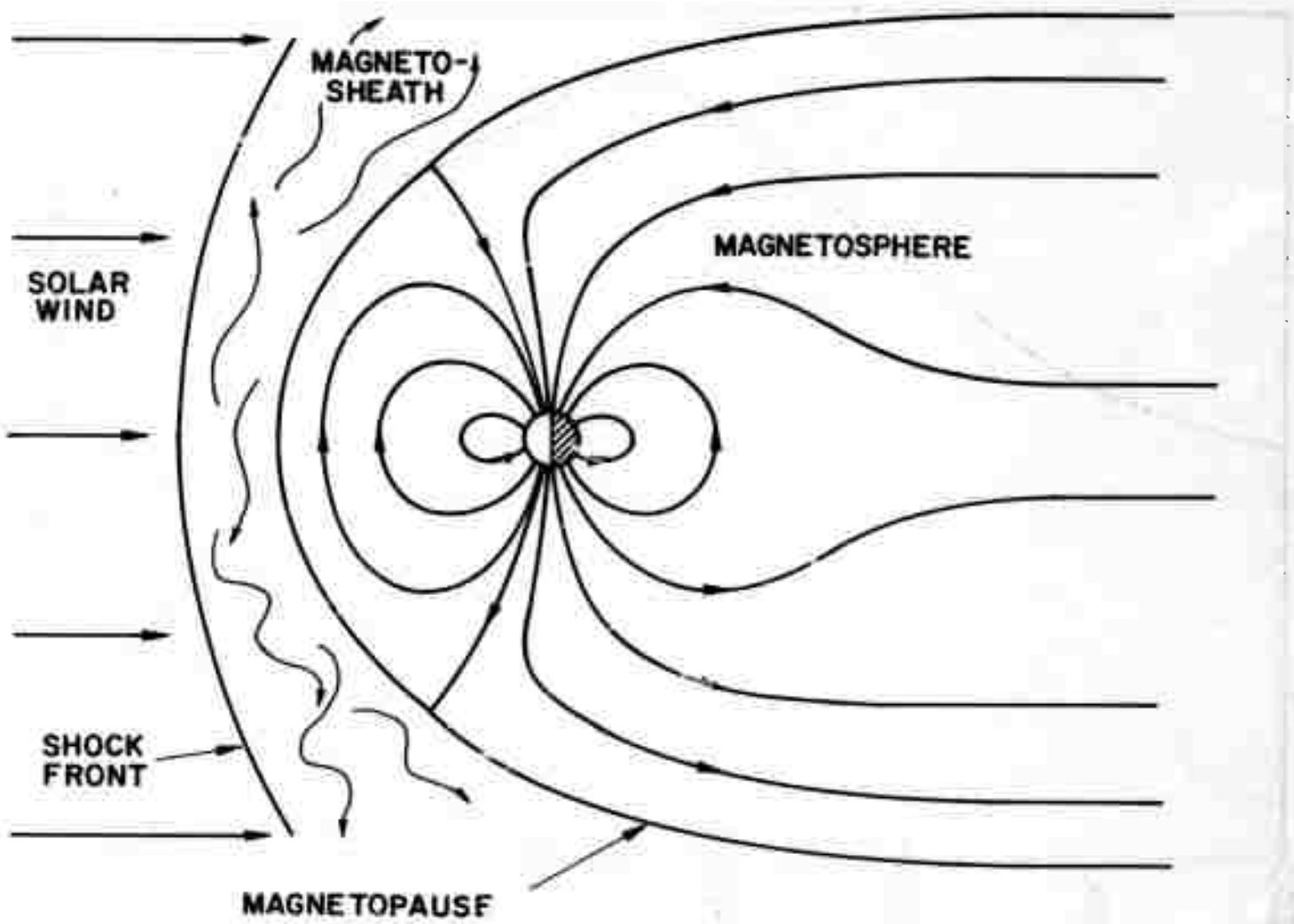

Figure 11. A simplified view of the earth's magnetosphere, shown in cross-section perpendicular to the equatorial plane. This figure is adapted from Figure 61 of Rishbeth and Garriott (1969).

and thus the magnetosphere, end at about ten earth radii on the day side of the earth and farther out on the night side (see Figure 11).

APPENDIX C

DERIVATION OF EQUATION (1)

The development given here roughly parallels that given in Sections 5.3.1 and 5.3.2 of Clemmow and Dougherty (1969). Here, however, the effects of positive ions are included and some different notation is used.

We consider a plasma that is unbounded, cold, and collisionless, and that in the unperturbed state is uniform, neutral and at rest. All wave-field quantities are assumed to vary as $\exp(i\omega t - i\bar{k}\cdot\bar{r})$ where ω is the angular wave frequency, $\bar{k}$ is the vector wave number and $\bar{r}$ the position vector. For the electrons we can write down the linearized perturbational equation of motion as

$$i\omega m_e \bar{v}_e = -e(\bar{E} + \bar{v}_e \times \bar{B}_o) \quad .$$

Here m_e is the mass, $-e$ is the charge, $\bar{v}_e$ is the perturbation velocity, $\bar{E}$ is the average electric field and $\bar{B}_o$ the static magnetic field. An analagous equation describes the ion motion. Now letting $\bar{B}_o = (0,0,B_o)$ and noting that the perturbation current is $\bar{j} = Ne(\bar{v}_i - \bar{v}_e)$ for assumed-equal unperturbed number densities N of electrons and ions, the x component of the current can be written as

$$j_x = \epsilon_o \frac{\omega_{pe}^2}{\omega^2 - \omega_{ce}^2}(\omega_{ce}E_y - i\omega E_x) - \epsilon_o \frac{\omega_{pi}^2}{\omega^2 - \omega_{ci}^2}(\omega_{ci}E_y + i\omega E_x)$$

with similar expressions for j_y and j_z. Here $\omega_{pe} = (Ne^2/\epsilon_o m_e)^{1/2}$ is the electron plasma frequency and $\omega_{ce} = e B_o/m_e$ is the electron gyro frequency. Again there are similar definitions for ω_{pi} and ω_{ci} with only the mass subscripts changed.

Maxwell's equation for the curl of the average time-varying magnetic field $\bar{B}$ is

$$\nabla \times \bar{B} = \mu_o \bar{j} + i\omega\mu_o\epsilon_o\bar{E} \triangleq i\omega\mu_o\epsilon_o \hat{\epsilon} \cdot \bar{E}$$

Preceding page blank

where μ_o and ϵ_o are the free-space permeability and permittivity respectively, and $\hat{\epsilon}$ is defined to be the equivalent relative-permittivity tensor of the medium. Substituting for $\bar{j}$ and solving for $\hat{\epsilon}$ we obtain

$$\hat{\epsilon} = \begin{bmatrix} \epsilon_\perp & -i\epsilon_x & 0 \\ i\epsilon_x & \epsilon_\perp & 0 \\ 0 & 0 & \epsilon_\parallel \end{bmatrix}$$

where

$$\epsilon_\perp = 1 - \frac{\omega_{pe}^2}{\omega^2 - \omega_{ce}^2} - \frac{\omega_{pi}^2}{\omega^2 - \omega_{ci}^2} \quad ,$$

$$\epsilon_x = \frac{\omega_{ce}}{\omega} \cdot \frac{\omega_{pe}^2}{\omega^2 - \omega_{ce}^2} - \frac{\omega_{ci}}{\omega} \cdot \frac{\omega_{pi}^2}{\omega^2 - \omega_{ci}^2} \quad ,$$

and

$$\epsilon_\parallel = 1 - \frac{\omega_{pe}^2}{\omega^2} - \frac{\omega_{pi}^2}{\omega^2} \quad .$$

The Maxwell curl equations are now

$$\nabla \times \bar{E} = -i\omega\bar{B}$$

and

$$\nabla \times \bar{B} = i\omega\mu_o\epsilon_o\hat{\epsilon}\cdot\bar{E} \quad .$$

Eliminating $\bar{B}$ and performing some algebra we obtain the wave equation

$$k^2\bar{E} - \bar{k}(\bar{k}\cdot\bar{E}) - k_o^2\,\hat{\epsilon}\cdot\bar{E} = 0$$

where $k_o = \omega/c$ is the free space wave number. Restricting $\bar{k}$ to lie in the x-z plane and writing out this last equation by components we obtain

$$\begin{bmatrix} k_z^2 - \epsilon_\perp k_o^2 & i\epsilon_x k_o^2 & -k_x k_z \\ -i\epsilon_x k_o^2 & k_x^2 + k_z^2 - \epsilon_\perp k_o^2 & 0 \\ -k_x k_z & 0 & k_x^2 - \epsilon_\parallel k_o^2 \end{bmatrix} \begin{bmatrix} E_x \\ E_y \\ E_z \end{bmatrix} = 0 \quad .$$

Dividing through by $-k_o^2$ and noting that $k_x = k_o\, n \sin\theta$ and $k_z = k_o\, n \cos\theta$, where n is the refractive index and θ is the angle between $\bar{k}$ and $\bar{B}_o$, this equation becomes

$$\begin{bmatrix} \epsilon_\perp - n^2\cos^2\theta & -i\epsilon_x & n^2\sin\theta\cos\theta \\ i\epsilon_x & \epsilon_\perp - n^2 & 0 \\ n^2\sin\theta\cos\theta & 0 & \epsilon_\parallel - n^2\sin^2\theta \end{bmatrix} \begin{bmatrix} E_x \\ E_y \\ E_z \end{bmatrix} = 0$$

which is equation (1) of the text.

Note that for the low-frequency case where $\omega \ll \omega_{ci}$, the following approximations can be made:

$$\epsilon_x \approx 0$$

and

$$\epsilon_\perp \approx \frac{\omega_{pi}^2}{\omega_{ci}^2} = \frac{Nm_i}{\epsilon_o B_o} = \frac{c^2}{v_A^2} \quad .$$

Here c is the vacuum speed of light and v_A is the Alfvén speed defined by $v_A^2 = B_o^2/\mu_o N m_i$. It has been assumed that $v_A^2 \ll c^2$ as is the case in the F region of the ionosphere.

REFERENCES

Budden, K. G., Radio Waves in the Ionosphere, The University Press, Cambridge, 1961.

Carlson, A. B., Communication Systems, McGraw-Hill, New York, 1968.

Chapman, S. and J. Bartels, Geomagnetism, II, The Clarendon Press, Oxford, 1940.

Clemmow, P. C. and J. P. Dougherty, Electrodynamics of Particles and Plasmas, Addison-Wesley, London, 1969.

Fraser-Smith, A. C., Possible direct detection of Pc 1 micropulsation propagation in the F_2-region ionospheric duct by HF radio sounding, Trans. A. G. U., 50, 651, 1969.

Greifinger, C. and P. S. Greifinger, Theory of hydromagnetic propagation in the ionospheric waveguide, J. Geophys. Res., 73, 7473, 1968.

Jacobs, J. A., Geomagnetic Micropulsations, Springer-Verlag, Heidelberg, 1970.

Rishbeth, H. and O. K. Garriott, Introduction to Ionospheric Physics, Academic Press, New York, 1969.

Utlaut, W. F. and R. Cohen, Modifying the ionosphere with intense radio waves, Science, 174, 245, 15 October 1971.